

# Origami Sensitivity – Rigid Foldability, Feasibility, and Geometry Optimization of an Adapted Flasher

L. Zimmermann, K. Shea, T. Stanković

keywords: origami sensitivity, rigid foldability, origami geometry optimization

## Abstract

The computational generation of origami crease patterns has so far focused mainly on the artistic realm (*A computational algorithm for origami design*, R.J. Lang, 1996) or corrugated surfaces (*Origamizing Polyhedral Surfaces*, T. Tachi, 2010), which both exhibit limited use for engineering applications. The complexity of origami generation stems from both geometry and topology of crease patterns, which directly determine the kinematic behavior of an origami. The present work takes a step towards origami generation but reduces the complexity by focusing only on the influence of pattern geometry, assuming a valid topology is known. The contribution is a general approach for origami geometry optimization that is based on the simulation and analysis of underlying search spaces. The analysis is performed within a case study of an adapted flasher, and includes an assessment of rigid foldability as well as spatial feasibility, which consists of facet intersection and space restrictions for the folded state.

The case study involves the previously unknown, four-symmetrical, two-layered, and rigid-foldable flasher shown in Fig. 1 (left). The rigid foldability, resulting from introducing the additional crease lines depicted as dashed lines, is presented without proof but is verified through numerical simulation. One attribute flasher-type structures have in common is that each time an inner layer (Fig. 1 left) is fully folded (Fig. 1 right), the folding motion must be continued by activating outer layers. The goal of the case study is thus to find a geometrical variation of the rigid-foldable flasher whose folded state fits into the cuboid ( $-1 \leq x, y \leq 1, -4 \leq z \leq 0$ ) in Fig. 1 (right) once facets  $f_2$  are folded  $90^\circ$  around  $f_1$ , while maintaining a near-flat and maximally large surface in the beginning.

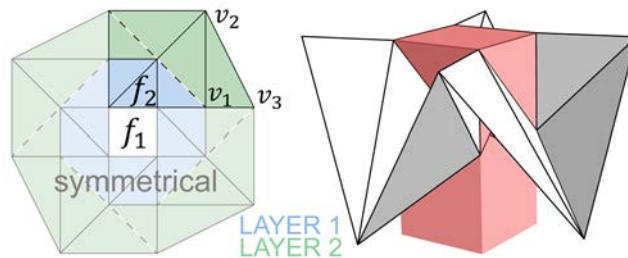


**Figure 1:** Added dashed crease lines result in rigid-foldable flasher pattern (left) whose folded configuration should fit into the cuboid shown in red (right).

A prerequisite for a generally applicable optimization is the possibility to kinematically simulate the whole range from stretching/bending to rigid foldable patterns. For this purpose,

the constraints of a previously presented simulator for rigid-foldable origami (*Finding Rigid Body Modes of Rigid-Foldable Origami Through the Simulation of Vertex Motion*, L. Zimmermann *et al.*, 2017) are relaxed to simulate any geometrical configuration. Eq. (1) shows the adapted folding condition, which is solved in each simulation step, in terms of vertex positions  $\mathbf{x}$ . The absolutes of the differences between  $n$  actual and target constraint lengths,  $\mathbf{l}_a$  and  $\mathbf{l}_t$  respectively, have to be smaller or equal to values  $\epsilon$  whose sum  $E$  is then minimized.

$$\min_{\mathbf{x}} \left\{ E = \sum_{i=1}^n \epsilon_i \mid |\mathbf{l}_a - \mathbf{l}_t| \leq \epsilon \right\} \quad (1)$$

With this adaptation, search spaces are first investigated for *Layer 1* of the rigid-foldable flasher, after which conclusions are drawn for the optimization of *Layer 2*. Fig. 2 shows the influence of the starting position of vertex  $v_1$  – the only vertex with unknown motion in *Layer 1* – on its own folding behavior. The variation of the position of  $v_1$  *before* folding constitutes the axes of all plots in Fig 2. The top row (2.a-c) shows the position of  $v_1$  in  $x$ ,  $y$  and  $z$  *after* folding. The bottom row (2.d-f) depicts the rigidity error, i.e.  $E$  averaged over all simulation steps, the intersection of facets during folding, and the feasible solutions when all plots are superimposed, respectively.

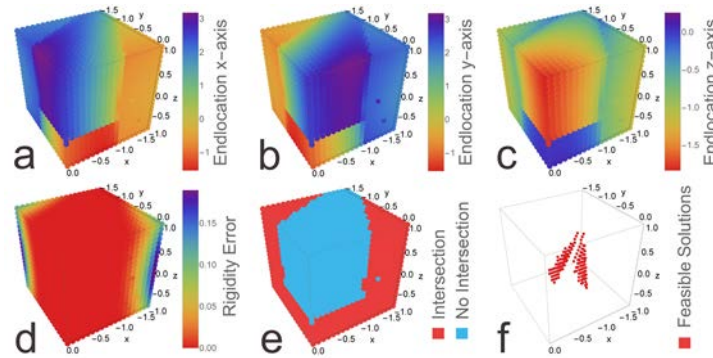


**Figure 2:** Influence of the starting location of  $v_1$ : Its end location in  $x$ ,  $y$  and  $z$  (a-c), and rigidity error, intersection, and feasible solutions (d-f), respectively.

The results concerning the vertex end location (2.a-c) show that there exist different sub-domains, within which the behavior is monotonic. The same monotonicity can be observed (symmetrically) for the rigidity error (2.d), whereas the intersection (2.e) is binary, but domain-specific. Hence, these properties can all be embedded into the objective function of the case study (maximum area with minimum deflection from horizontal plane) as either penalty (end location and rigidity error) or boundary (intersection) functions, and solved by the Nelder-Mead method, applied globally. A detailed description of the optimization will be demonstrated in the full paper. The outcome is an optimized adapted flasher, as shown in Fig. 3.



**Figure 3:** Discrete folding states of the optimized adapted flasher.